

Available online at [www.sciencedirect.com](http://www.sciencedirect.com)

ScienceDirect



St. Petersburg Polytechnical University Journal: Physics and Mathematics 2 (2016) 150–156

[www.elsevier.com/locate/spjpm](http://www.elsevier.com/locate/spjpm)

# The borders of existence of anomalous convection flow in the inclined square cylinder: Numerical determination

Albert N. Sharifulin<sup>a,\*</sup>, Anatoliy N. Poludnitsin<sup>b</sup><sup>a</sup> Perm National Research Polytechnic University, 29 Komsomolsky Ave., Perm, 614990, Russian Federation<sup>b</sup> Perm State University, 15 Bukireva St., Perm, 614113, Russian Federation

Available online 27 May 2016

## Abstract

The article is dedicated to the study of bifurcations of stationary convection regimes in a closed, heated from below and tilted square cylinder filled with air for cases of heat-insulated and perfectly heat-conducting sidewalls. The temperature and velocity fields were obtained using grid method for inclinations from a horizontal position up to 30 degrees in the range of Rayleigh numbers up to 20-fold excess of its critical value. The limit angle of anomalous-flow existence in the cylinder with the heat-insulated walls was established to be about 3 times greater than that in the cylinder with the heat-conducting ones. In the case of the heat-conducting walls the maximum angle of the anomalous-flow existence reached 7.7 degrees at a 3.3-fold excess of the critical value of Rayleigh number.

Copyright © 2016, St. Petersburg Polytechnic University. Production and hosting by Elsevier B.V.

This is an open access article under the CC BY-NC-ND license. (<http://creativecommons.org/licenses/by-nc-nd/4.0/>)**Keywords:** Thermal convection; Inclination of the cavity; Anomalous flow; Numerical simulation.

## Introduction

Thermal air convection in closed and tilted rectangular cavities is of interest due to the fact that containers of this type are the elements in a great number of technical devices. Their orientation can change smoothly or stepwise, while the convective flows in the gas filling the volume can undergo abrupt changes [1].

A cube is often used for simulating the effect of tilting on the convection modes in a closed rectangular cavity. At low and moderate Rayleigh numbers

(Ra), convective air flows in the cube have the form of single-roll flows, i.e., of vortices with horizontal axes. Liquid particles in these flows are moving along circular paths in planes perpendicular to the vortex axis. Such a flow near the central vertical section of a cube can be considered quasi-two-dimensional [2]. This circumstance allows to expect a numerical study of 2D air flows, i.e., of infinitely extended horizontal vortices, in abstract infinite cylinders to provide insights into the observed bifurcation patterns of stationary convection regimes in laboratory experiments with a cubic cavity. The first numerical study on the influence of tilting (rotation of an infinite square cross-section cylinder around the axis) on the heat transfer between opposite isothermal walls (the other two walls

\* Corresponding author.

E-mail addresses: [sharifulin@bk.ru](mailto:sharifulin@bk.ru) (A.N. Sharifulin), [panam.48@mail.ru](mailto:panam.48@mail.ru) (A.N. Poludnitsin).<http://dx.doi.org/10.1016/j.spjpm.2016.05.013>2405-7223/Copyright © 2016, St. Petersburg Polytechnic University. Production and hosting by Elsevier B.V. This is an open access article under the CC BY-NC-ND license. (<http://creativecommons.org/licenses/by-nc-nd/4.0/>) (Peer review under responsibility of St. Petersburg Polytechnic University).

were assumed to be heat-insulated) was carried out by Polezhaev [3]. This study established that the maximal heat flow was achieved at an intermediate tilt angle, i.e., between the heating from below and from the side.

The first data on the bifurcation of the convective air flow in a cubic cavity heated from below, caused by tilting, were published in the experimental study [4], which only considered small tilt angles, i.e., for the position corresponding to the heating strictly from below. It should be explained here that tilting at low  $Ra$  numbers results in the formation of a vortex with the circulation direction coinciding with the direction of the tilt angle of the cavity (if we regard the tilt angle as the rotation of the cavity from a zero angle). This vortex has normal circulation, and it stops rotating if the cavity is brought into a horizontal position. However, at Rayleigh numbers exceeding the critical value ( $Ra_c$ ), it is possible for a vortex with a reverse circulation direction to coexist with the normal vortex. The term ‘anomalous’ was suggested for such flows in Ref. [5]. The directions of air circulation and of the cavity’s tilt angle are opposite in an anomalous vortex, which means that the warm air flows downward along the tilted surface. Anomalous vortices exist within a certain range of tilt angles; the width of this range depends on the intensity of the convective flow. The experimental boundaries within which anomalous convective flow exists in a cube were experimentally determined in Ref. [6].

The goal of this study is in constructing a bifurcation curve reflecting the relationship between the critical tilt angle at which an anomalous vortex exists and the intensity of the convective flow.

The construction process should be based on numerically solving the full equations of thermal air convection (in the Boussinesq approximation) for different tilt angles of a square cavity and various critical parameter values.

### Problem setting

Suppose that liquid fills a cavity shaped as an infinite horizontal cylinder of square cross-section (Fig. 1). Let us introduce a Cartesian coordinate system  $(x, y, z)$  whose  $y$ -axis coincides with an edge of the cylinder and is directed away from us. The unit vector  $\mathbf{n}$  is located in the  $xz$  plane, points upward and is connected with the acceleration of gravity by the ratio  $\mathbf{g} = -g\mathbf{n}$ . The tilt angle of the square cylinder  $\alpha$  is measured clockwise between the  $z$ -axis and  $\mathbf{n}$ . The variation range of the  $\alpha$  angle in the calculations

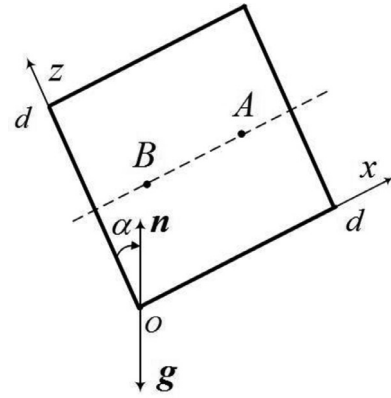


Fig. 1. Geometry of the problem on free thermal convection in a horizontal square cross-section cylinder.

The mean cross-section, marked by a dashed line, contains the points  $A$  and  $B$  between which the temperature difference  $dT$  is calculated. These points are located at a distance  $d/4$  from the side-walls (see the explanations in the text).

is  $-30^\circ \leq \alpha \leq 30^\circ$ ; at  $\alpha = 0^\circ$  the side of the cylinder coinciding with the  $x$  axis is horizontal, with the heating strictly from below. Fig. 1 shows the height-average square cross-section, with the points  $A$  and  $B$  marked; the temperature difference between these points is calculated for comparing the numerical results with the thermocouple measurements in a laboratory experiment [6].

The cavity walls are assumed to be solid. The upper and lower planes  $z=0, d$  are isothermal and maintained at a constant temperature difference  $\Theta$ , with the  $z=0$  plane the more heated. The calculations used two cavity models in which the sidewalls  $x=0, d$  are assumed to be either heat-conducting (a linear temperature distribution  $T = \Theta(1 - z/d)$  is then given on them), or insulated (the equality  $\partial T / \partial x = 0$  then describes the lack of heat flow through the surface). The linear expansion coefficient of the liquid  $\beta$ , the kinematic viscosity  $\nu$  and the thermal diffusivity  $\chi$  are constant.

It is assumed that the fluid is incompressible, and that the Boussinesq approximation holds true. The velocity  $\mathbf{v}$ , the pressure  $p$  and the temperature  $T$  are determined by the continuity equations, by the Navier–Stokes, and the heat balance equations. Let us denote the distance, the temperature, and the flow and time functions as, respectively,  $d, \Theta$ , the kinematic viscosity  $\nu$  and  $d^2/\nu$ . We shall seek for two-dimensional solutions of the problem. In this case, the vector fields of vorticity and flow function will differ from zero only in the  $y$ -components:

$$\vec{\varphi} = (0, \varphi, 0), \quad \vec{\psi} = (0, \psi, 0). \quad (1)$$

The thermal convection equations in dimensionless form are then written as [7,8]:

$$\frac{\partial \varphi}{\partial t} + \frac{\partial \psi}{\partial x} \frac{\partial \varphi}{\partial z} - \frac{\partial \psi}{\partial z} \frac{\partial \varphi}{\partial x} = \frac{\partial^2 \varphi}{\partial x^2} + \frac{\partial^2 \varphi}{\partial z^2} + \text{Gr} \left( \frac{\partial T}{\partial z} \sin \alpha - \frac{\partial T}{\partial x} \cos \alpha \right); \quad (2)$$

$$\frac{\partial^2 \psi}{\partial x^2} + \frac{\partial^2 \psi}{\partial z^2} + \varphi = 0; \quad (3)$$

$$\frac{\partial T}{\partial t} + \frac{\partial \psi}{\partial x} \frac{\partial T}{\partial z} - \frac{\partial \psi}{\partial z} \frac{\partial T}{\partial x} = \frac{1}{\text{Pr}} \left( \frac{\partial^2 T}{\partial x^2} + \frac{\partial^2 T}{\partial z^2} \right). \quad (4)$$

The dimensionless similarity criteria, namely the Grashof number Gr, the Prandtl number Pr and the Rayleigh number Ra have the form:

$$\text{Gr} = \frac{g\beta\Theta d^3}{\nu^2}, \quad \text{Pr} = \frac{\nu}{\chi}, \quad \text{Ra} = \text{Gr} \cdot \text{Pr}. \quad (5)$$

The flow velocity is related to the flow function field  $\psi(x, z)$ :

$$\mathbf{v} = \left( -\frac{\partial \psi}{\partial z}, 0, \frac{\partial \psi}{\partial x} \right). \quad (6)$$

The boundary conditions for the temperature at the isothermal top and bottom walls are written in the following form:

$$\text{if } z = 0, 1 \quad T = 1, 0. \quad (7)$$

The boundary conditions for the temperature in the case of the conducting sidewalls with the linear temperature distribution had the form:

$$\text{if } x = 0, 1 \quad T = 1 - z. \quad (8)$$

A no-heat-flow condition was imposed for the heat-insulated sidewalls:

$$\text{if } x = 0, 1 \quad \frac{\partial T}{\partial x} = 0. \quad (9)$$

The boundary conditions for the flow function were identical in both cases. The cavity walls were assumed to be impermeable and solid. The wall impermeability and no-slip conditions generate the boundary conditions for the flow functions:

$$\text{if } z = 0, 1 \quad \psi = \frac{\partial \psi}{\partial z} = 0; \quad (10)$$

$$\text{if } x = 0, 1 \quad \psi = \frac{\partial \psi}{\partial x} = 0. \quad (11)$$

## The procedures for solving the problem and for the calculations

The solution for the problem given by equations and conditions (2)–(11) was found by the finite-difference method. The Prandtl number was set to equal 0.7. The calculations were performed on a uniform square grid:

$$x_i = i \cdot h, \quad z_k = k \cdot h, \\ i = 0, 1, \dots, N; \quad k = 0, 1, \dots, N;$$

where  $h = 1/N$  is the grid step. All calculations were performed for  $N=40$ .

We used the explicit scheme with central differences for the spatial derivatives [7]. The Thom formula was used to approximate the vorticity at the boundaries. The size of the time step  $\Delta t$  was controlled and chosen to be sufficiently small in order to satisfy the Courant condition.

Let us describe the procedure for obtaining the solution for the given values of the Grashof number Gr and the angle  $\alpha$ .

**Step 1.** Let us set the initial conditions for the temperature, the flow function and the vorticity in all nodes of the grid on the first temporal layer, i.e., at time  $t=0$ :

$$T_{i,k}^0 = 1 - z_k,$$

$$\psi_{i,k}^0 = 0,$$

$$\varphi_{i,k}^0 = 0,$$

Let us set the number of the temporal layer  $n=0$ .

**Step 2.** Assuming  $T^n$  and  $\varphi^n$  to be known, we find the values of these functions from the finite-difference equivalents of Eqs. (2) and (4) on the temporal layer  $n+1$  in the internal nodes of the grid. In the case of heat-insulated walls we substitute the boundary temperature value with the temperature value in the adjacent inner node.

**Step 3.** By solving Poisson's Eq. (3) from the calculated  $\varphi^{n+1}$  values, we obtain  $\psi^{n+1}$  in the internal nodes of the grid.

**Step 4.** By using the new flow function values in the boundary nodes, we obtain the limit values for the vorticity at the new time step.

Steps 2–4 are repeated until steady-state values of  $T$  and  $\psi$  are obtained. The values of these grid functions along with the physical and numerical parameters for the given value of the Grashof number Gr and the tilt angle  $\alpha$  are stored in the external memory. Step 1 was

omitted upon moving on to the next value of the angle  $\alpha$ , and the previously obtained state was used as the initial one.

The goal of the calculations was to obtain bifurcation curves  $dT(\alpha)$  and  $\psi_c(\alpha)$ . Here  $\psi_c$  is the maximum value of the flow function and  $dT$  is the temperature difference between the points *A* and *B* and (see Fig. 1). The tilt angle in the calculations changed successively with a variable step  $\Delta\alpha = 1\text{--}10^\circ$  from the initial value  $\alpha = -30^\circ$  to the final value  $\alpha = +30^\circ$  and back.

### Calculation results and discussion

In order to perform the main calculations in accordance with the above-described procedure, we carried out a test of the model used and of the difference method. For this purpose, we calculated the critical Grashof numbers under heating strictly from below ( $\alpha = 0^\circ$ ), and then compared them with the standard values obtained by the methods of linear stability theory. The method for obtaining the critical Grashof number was based on extrapolating the linear dependence of the squared flow function on the Grashof numbers towards lower values. The critical Grashof numbers for the heat-conducting walls ( $Gr_c = 7156$ ) and the heat-insulated ones ( $Gr_c = 3643$ ) were obtained this way.

It is known that the critical Rayleigh number for the heat-conducting walls is  $Ra_c = 5012$  [9], and the corresponding critical Grashof number at  $Pr = 0.7$  is equal to 7160. For the heat-insulated cavity walls the critical Grashof number is equal to 3693 [10,11]. Thus, it was revealed as a result of the test calculations that the critical Grashof numbers obtained are different from those determined by the methods of linear stability theory by less than 1.5%, indicating a satisfactory accuracy of the numerical method used.

Since different boundary conditions correspond to different critical Grashof numbers, we used the concept of the critical parameter; it was expressed by the ratio  $r = Gr / Gr_c$ .

The behavior of the convective roll flow under normal and anomalous conditions determined by the tilt angle of the cavity is, without a doubt, an interesting study subject. A flow that keeps circulating when the cavity tilt angle passes through zero is customarily called anomalous. [5] The intensity and direction of the circulation of a two-dimensional roll flow under steady conditions is explicitly described by the extreme value of the flow function  $\psi_c(Gr, \alpha)$  in the center of the cavity, i.e., the phase space of the sys-

tem is one-dimensional. The thermal convection at the zero angle  $\alpha = 0$  develops smoothly as a result of fork bifurcation on the  $\psi_c(Gr)$  plane at the critical Grashof number  $Gr_c$ . However, even a slight tilt (about 0.01 degrees [12]) leads to convection appearing at any arbitrarily small values of the Grashof number.

Calculations showed that the convective roll flow that developed at a cavity tilt angle differing from zero, and at a fixed Grashof number less than or equal to the critical one ( $r \leq 1$ ), reverses its direction smoothly when the cavity tilt angle  $\alpha$  passes through zero (solid line in Fig. 2). If the Grashof number exceeds the critical value ( $r > 1$ ), the convective roll flow preserves the direction of movement when the cavity tilt angle passes through zero, thus becoming anomalous. This flow persists up to a certain critical angle  $\alpha_c$ ; upon reaching this angle, it abruptly reverses its direction and turns into a normal flow. Bifurcation diagrams for  $\psi_c(\alpha)$ , obtained through the calculations for four values of  $r$ , illustrate this behavior (see Fig. 2).

Curves 1–4 in Fig. 2 correspond to the different values of the critical parameter. The crosses correspond to the successive changes in the tilt of the cavity from the negative to the positive angles, and the squares from the positive to the negative angles. Bifurcation diagrams indicate the existence of an anomalous flow, which, however, transforms into a normal one when the tilt angle reaches the critical value  $\alpha_c$ . The existence region of the anomalous flow broadens with an increase in the value of the critical parameter. As can be seen from Fig. 2, for each  $\alpha$  from the  $-\alpha_c < \alpha < \alpha_c$  interval, there are two steady states which differ by their circulation direction, i.e., by the sign of  $\psi_c$ .

Experimental studies of convection in cavities with heat-conducting walls typically include measurements by thermocouples [1,4,6]. The data from the differential thermocouples installed in specific locations in the cavity allows to assess the structure of the convective flow. In the works mentioned the thermocouple junctions were located in points *A* and *B* (see Fig. 1). The values of the dimensionless temperature difference  $dT$  read from such a virtual thermocouple are shown in Fig. 3 as a function of the cavity tilt angle for four values of the critical parameter  $r$ . We can see that the jump changes of  $dT$  and  $\psi_c$  for the same values of  $r$  occur at the same tilt angles (see Fig. 2).

The evolution of the temperature fields and the flow lines with a change of the cavity tilt angle  $\alpha$  from  $+30^\circ$  to  $-30^\circ$  for  $r = 2.5$  is presented in Fig. 4. For

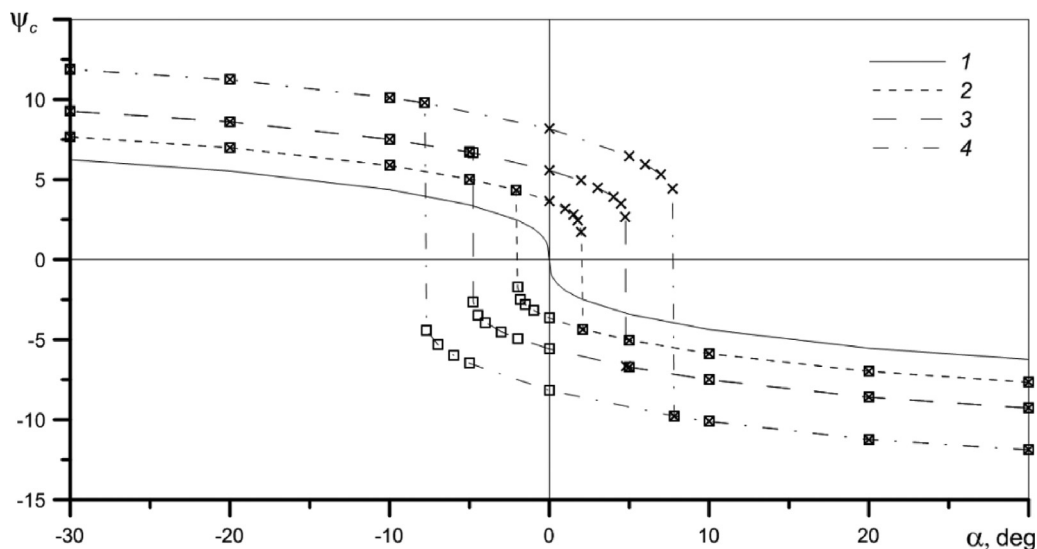


Fig. 2. Flow function  $\psi_c$  in the center of the cavity versus the cavity tilt angle  $\alpha$  for the case of heat-conducting walls at different values of the critical parameter  $r$ : 1.0 (curve 1), 1.3 (2) 1.7 (3) 2.5 (4).

Crosses (squares) indicate the diagrams obtained under the variation of the  $\alpha$  angle from  $-30^\circ$  to  $+30^\circ$  (from  $+30^\circ$  to  $-30^\circ$ ) (see the explanations in the text).

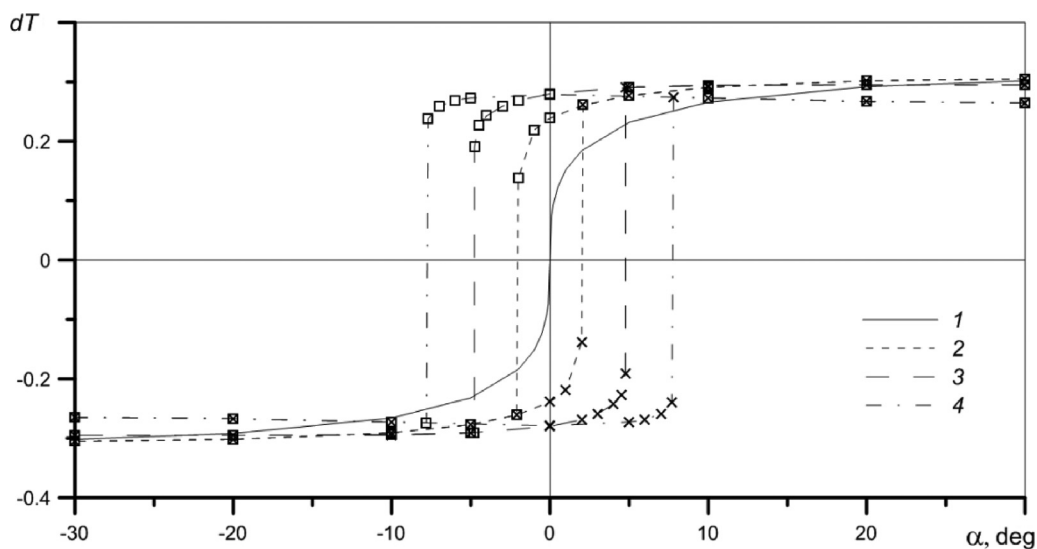


Fig. 3. Temperature difference  $dT$  between the points  $A$  and  $B$  versus the cavity tilt angle  $\alpha$  for the case of heat-conducting walls at different values of the critical parameter  $r$  (curve symbols and numbers are the same as in Fig. 2).

the normal flow in the variation range of the angle  $\alpha$  from  $+30^\circ$  to  $0^\circ$ , there is a gradual decrease in flow intensity (see curve 4 in Fig. 2), which continues to decrease after passing through zero; the structure of the flow is preserved. When the angle approaches the critical value  $\alpha_c = -7.8^\circ$ , the decrease in the intensity of the central vortex  $\psi_c$  accelerates, while corner vortices with the swirl opposite to that of the main vortex grow.

The transition process happens in the following manner. One of the corner vortices grows faster than the other one which then disappears. The growing vortex (which has a normal rotation direction at the given tilt angle) displaces the anomalous one. Images of the flow function and the isotherms for the critical angle of  $\alpha_c = -7.8^\circ$  are provided for two times. The first time corresponds to the moment of the change of the flow structure, and the second one to the moment when the



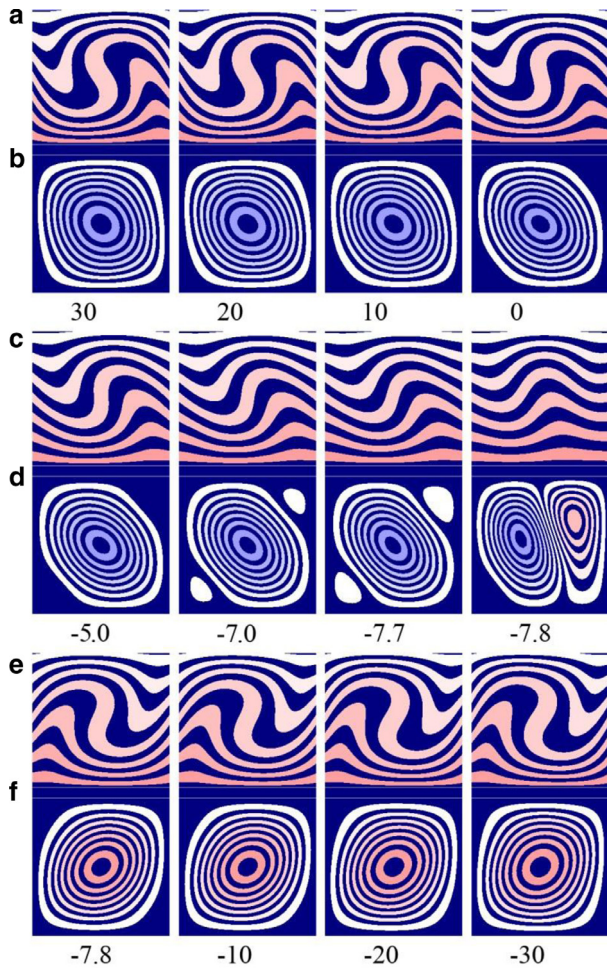


Fig. 4. The evolution of the temperature field (a, c, e) and the flow structure (b, d, f) for the case of heat-conducting walls with a change of the tilt angle  $\alpha$  from  $+30^\circ$  to  $-30^\circ$ ;  $r=2.5$ . The figures represent the tilt angles  $\alpha$ . The boundaries of the seven isotherms in the figure (a, c, e) correspond to fourteen temperature values:  $T_j = (2j - 1)/28$ , while the boundaries of the flow lines (b, d, f) correspond to  $|\psi_j| = \psi_c \cdot (2j - 1)/28$ , where  $j = 1, 2, \dots, 14$ .

transition process has been completed. The images below describe the evolution of the normal vortex chamber up to the angle  $\alpha = -30^\circ$ . The tilt angle changing in the reverse direction results in obtaining a critical angle with a value equal to  $\alpha_c = +7.8^\circ$  in the positive angle range.

The results of the calculations performed for two cases of boundary conditions for the temperature are presented as bifurcation curves in Fig. 5. For the heat-conducting walls (curve 1) this curve has a pronounced maximum  $\alpha_c = 7.7^\circ$  at  $r = 3.3$ . These values are close to those obtained in the calculations of the bifurcation curve for a circular cylinder with heat-conducting

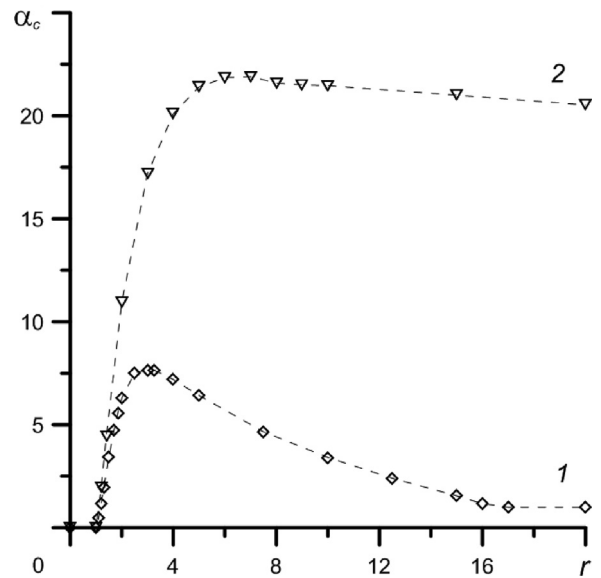


Fig. 5. Critical angles versus the critical parameter values for the cases of heat-conducting (curve 1) and heat-insulated (curve 2) walls.

walls [13,14], but still differ from them. The bifurcation curve for the heat-insulated walls corresponds to the results obtained in Refs. [15,16]. The calculations in [15] were carried out by the Petrov–Galerkin method, which used up to seventy basis functions. Chebyshev polynomials served as these functions. The individual points of the bifurcation curves for three Prandtl numbers obtained in [16] are consistent with the results of Ref. [15] for the case of the air. Our calculations, performed on a relatively coarse grid, yielded good agreement with the results presented in Ref. [15], which indicates the reliability of our findings.

## Conclusion

This paper has presented a numerical study of anomalous flow in the square cross-section cylinder, with bifurcation curves obtained for the cases of heat-conducting and heat-insulated sidewalls.

It was established that the limit angle for the existence of anomalous flow in the case of heat-insulated walls was about three times greater than that for the heat-conducting walls. Thus, in the case of heat-conducting walls, the transition from normal to anomalous flow occurs at a smaller cavity tilt angle and at a lower value of the critical parameter.

The bifurcation diagrams of the flow function and the temperature difference versus the tilt angle show

identical values of the critical tilt angle at which the convective roll flow changes direction with the same value of the critical parameter. This means that thermocouple measurement results could be used in experimental studies of anomalous convective roll flows for determining the critical tilt angle of the cavity (the angle at which the flow changes direction).

It follows from the calculations that the change in the rotation direction occurs as a result of intense growth of one of the normal diagonal vortices, which suppresses and displaces the anomalous convective roll.

The study was carried out with the financial support of an intra-university grant of the Perm National Research Polytechnic University

## References

- [1] A.N. Sharifulin, A.N. Poludnitsin, A.S. Kravchuk, Laboratory-scale simulation of nonlocal generation of a tropical cyclone, *JETP* 107 (6) (2008) 1090–11093.
- [2] J. Mizushima, O. Matsuda, Onset of 3D thermal convection in a cubic cavity, *J. Phys. Soc. Jpn.* 66 (8) (1997) 2337–2341.
- [3] V.I. Polezhaev, *Tekhnika i teploobmen pri yestestvennoy konveksii gaza v zamknutoy oblasti posle poteri ustoychivosti gidrostaticheskogo ravnovesiya* [Flow and heat transfer with natural convection of a gas in a closed region after loss of hydrostatic equilibrium stability], *Izv. AS USSR* 5 (1968) 124–129.
- [4] V.D. Zimin, A.I. Ketov, *Nadkriticheskiye konvektivnyye dvizheniya v kubicheskoy polosti* [Supercritical convective motions in a cubic cavity], *Izv. AS USSR, Mech. Fluid Gases* 5 (1974) 110–114.
- [5] K.A. Cliffe, K.H. Winters, A numerical study of the cusp catastrophe for Benard convection in tilted cavities, *J. Comp. Phys.* 54 (3) (1984) 531–534.
- [6] A.N. Sharifulin, A.N. Poludnitsin, Experimental determination of limits of existence of anomalous convective currents in tilted cube, *J. Appl. Mech. and Techn. Phys* 55 (3) (2014) 462–469.
- [7] E.L. Tarunin, *Vychislitelnyy eksperiment v zadachakh svobodnoy konveksii* [Numerical experiment in free convection problems], Irkutsk, Izd-vo Irkutskogo un-ta, 1990.
- [8] R.V. Sagitov, A.N. Sharifulin, Stability of steady state thermal convection in a titled rectangular cavity in low-mode approach, *Thermophysics & Aeromechanics* 15 (2) (2008) 233–241.
- [9] J. Mizushima, Y. Hara, Routes to unicellular convection in a tilted rectangular cavity, *J. Phys. Soc. Japan.* 69 (8) (2000) 2371–2374.
- [10] M. Lappa, *Thermal Convection: Patterns, Evolution and Stability*, Wiley, Chichester, 2010.
- [11] J. Mizushima, Onset of the thermal convection in a finite two-dimensional box, *J. Phys. Soc. Jpn.* 64 (7) (1995) 2420–2432.
- [12] T. Adachi, Stability of natural convection in an inclined square duct with perfectly conducting side walls, *Intern. J. Heat Mass Transf.* 49 (13) (2006) 2372–2380.
- [13] A.I. Nikitin, A.N. Sharifulin, Concerning the bifurcations of steady-state thermal convection regimes in a closed cavity due to the Whitney folding-type singularity, *Heat Transfer Soviet Research* 21 (2) (1989) 213–221.
- [14] D.A. Fominskiy, A.N. Sharifulin, Numerical determination of the borders for existence of anomalous convective flow in a cylinder tilted, *St. Petersburg State Polytech. Univ. J. Phys.Math* 2 (170) (2013) 191–196.
- [15] A.N. Sharifulin, S.A. Suslov, *Konvektivnyye bifurkatsii neszhimayemoy zhidkosti v naklonyayemoy polosti kvadratnogo secheniya* [Convective bifurcation of an incompressible fluid in a tilted square cavity], *Mater. 10th Intern. conf. “Vysokoproizvoditelnyye parallelnyye vychisleniya na klasternykh sistemakh” (NRS-2010)*, Perm, Nov. 1–3, 2010. Perm: Perm. Gos. Tekhn. Un-t. 2 (2010) 315–319.
- [16] V.I. Polezhaev, M.N. Myakshina, S.A. Nikitin, Heat transfer due to buoyancy-driven convective interaction in enclosures: fundamentals and applications, *Int. J. Heat Mass Transf.* 55 (1) (2012) 156–165.